SHORT COMMUNICATION
eISSN 2234-1757
Fish Aquat Sci. 2026;29(9):612-621
https://doi.org/10.47853/FAS.2026.e52
FAS Fisheries and Aquatic Sciences

Tissue recovery and amoxicillin residue depletion at alternative injection sites in olive flounder (*Paralichthys olivaceus*)

Ga-Won Kim[1,#], Hyo-Eun Lee[1,#], Joo-Won Hong[1], Mun-Gyeong Kwon[1], Ji-Hoon Lee[2,*], Jung-Soo Seo[1,*]

[1] *Aquatic Disease Control Division, National Fisheries Products Quality Management Service, Busan 49111, Korea*
[2] *Department of Aquatic Life Medicine, Kunsan National University, Gunsan 54150, Korea*

Abstract

Olive flounder (*Paralichthys olivaceus*) is a major aquaculture species in Korea, where amoxicillin is administered via intramuscular (IM) injection into the dorsal muscle for bacterial disease treatment. However, injection marks pose serious quality concerns in cultures where raw fish is consumed, resulting in a 34% price reduction in the Jeju region. This study compared traditional dorsal muscle injection with cheek muscle injection, a non-edible site, evaluating histopathological changes, drug residue concentrations, and pharmacokinetic/pharmacodynamic (PK/PD) characteristics. Olive flounder with an average body weight of 408.2 ± 35.7 g received IM injections of amoxicillin at 40 mg/kg into either dorsal or cheek muscle and were monitored for 480 hours. Histopathological analysis revealed hemorrhage, edema, necrosis, and inflammation at both injection sites, with complete tissue recovery not achieved even after the 20-day withdrawal period. High-performance liquid chromatography–tandem mass spectrometry (HPLC-MS/MS) analysis showed that cheek muscle reached maximum concentration at 3 hours while dorsal muscle peaked at 6 hours, with greater inter-individual variability observed in the cheek muscle group. PK/PD analysis demonstrated that cheek muscle injection provided higher systemic exposure in serum, whereas dorsal muscle injection showed advantages in local tissue drug retention. This study demonstrates that the current withdrawal period is sufficient for drug elimination but does not ensure complete recovery from injection-induced tissue damage. Changing the injection site to the non-edible cheek muscle represents a practical alternative that can address quality control issues while maintaining therapeutic efficacy.

Keywords: Olive flounder, Amoxicillin, Histopathology, Pharmacokinetics, Intramuscular injection

Received: Jan 7, 2026 **Revised:** Mar 1, 2026 **Accepted:** Apr 17, 2026
[#]These authors contributed equally to this work.
***Corresponding author:** Ji-Hoon Lee, Jung-Soo Seo
Department of Aquatic Life Medicine, Kunsan National University, Gunsan 54150, Korea
Aquatic Disease Control Division, National Fisheries Products Quality Management Service, Busan 49111, Korea
Tel: +82-63-469-1885, **E-mail:** jhlee01@kunsan.ac.kr, jsseosoo@korea.kr

Introduction

From 1961 to 2021, global seafood production experienced an average annual growth rate of 3%. By 2022, total production reached 185 million tonnes, with aquaculture contributing 94 million tonnes (51%), surpassing capture fisheries for the first time (FAO, 2024). This highlights the increasingly vital role of aquaculture in meeting the global demand for seafood. In the Korea, the olive flounder (*Paralichthys olivaceus*) is a premier aquaculture species. As of 2024, its production reached 40,125 tonnes, accounting for 55% of the total domestic fish aquaculture yield, with an economic value of approximately 684.2 billion KRW (Statistics Korea, 2025).

However, high-density aquaculture environments inevitably elevate the risk of infectious disease outbreaks (Krkošek, 2010), necessitating the continuous use of antibiotics. In 2015, total aquaculture antibiotic usage in Korea was 102,929 kg, of which amoxicillin, a broad-spectrum beta-lactam, was the most frequently utilized (15,594 kg, 15.5%) (Kim et al., 2019). For olive flounder, amoxicillin is typically administered via intramuscular (IM) injection at a dose of 40 mg/kg body weight (BW), which legally requires a 20-day withdrawal period to ensure food safety (NFQS, 2025).

Conventionally, withdrawal periods are established based solely on the depletion of antibiotic residues in edible muscle below acceptable safety thresholds. However, IM injections inherently cause mechanical and chemical tissue damage, leading to local inflammation and necrosis at the injection site (Abbate et al., 2018; Zoltick et al., 2024). If injection-induced lesions persist beyond the withdrawal period, they severely degrade fillet quality. This is particularly problematic in Korea and Japan, where olive flounder is predominantly consumed raw (sashimi). Visible injection marks have previously compromised consumer trust, notably causing a 34% price drop and a sharp decline in exports in Jeju, Korea (Ko, 2023; Park, 2019).

Despite these substantial economic impacts, research evaluating the histopathological recovery at injection sites during the withdrawal period remains scarce. It is currently uncertain whether the statutory 20-day withdrawal period guarantees complete tissue repair, highlighting the urgent need to evaluate alternative, non-edible IM injection sites. A recent pharmacokinetic study by Lee et al. (2023) established that administering amoxicillin via cheek muscle injection yields sufficient systemic serum exposure comparable to the traditional dorsal muscle injection, thereby validating its theoretical therapeutic efficacy against systemic infections. However, critical practical concerns regarding local tissue safety, site-specific absorption kinetics, and the extent of injection-induced histopathological damage have remained entirely unaddressed. Building directly upon the systemic PK framework provided by Lee et al. (2023), this short communication aimed to exclusively evaluate the local histopathological changes and muscle-specific PK characteristics during the withdrawal period following amoxicillin IM injection into both the edible dorsal muscle and the non-edible cheek muscle.

Material and Methods

Experimental animals

Olive flounder with an average BW of 408.2 ± 35.7 g were sourced from a private farm in Tongyeong, Gyeongsangnam-do, Korea. Fish weighing over 300 g were specifically selected to ensure sufficient cheek thickness for safe and accurate IM injection into the buccal region. The fish were acclimated for three weeks in 120-L flow-through tanks at 22 ± 0.5℃ and fed a commercial pellet diet (CJ Feed, Gunsan, Korea) at 1.5% of BW per day. Prior to drug administration, blood and muscle samples were collected from randomly selected fish to confirm the absence of amoxicillin residues. All experimental procedures were approved by the Institutional Animal Care and Use Committee (IACUC, NFQS-2022-6).

Drug preparation and administration

A commercial amoxicillin sodium formulation (AMOX injection, water-soluble powder, 50 g; KBNP Veterinary Medicine, Yesan, Korea) was reconstituted with phosphate-buffered physiological saline to achieve a final dose of 40 mg/kg BW. Intramuscular injections were administered using 1-mL syringes equipped with 3/16" × 23-gauge stainless steel veterinary needles (Socorex Isba SA, Ecublens, Switzerland), reflecting standard aquaculture practices to minimize tissue damage and ensure accurate drug delivery.

Experimental design

Olive flounder were randomly divided into two groups, each consisting of 70 fish. In a parallel design, one group received a single IM injection of amoxicillin at 40 mg/kg (a dose currently approved in Korea) into the dorsal muscle, while the other group was administered the same dose into the cheek muscle (Fig. 1). Muscle and skin were sampled from seven fish in both groups at each of the 0.5, 1, 3, 6, 12, 24, 48, 72, 168, and 480 hours post-

injection (hpi) time points. For these samples, tissue collection was performed after scale removal and included both skin and underlying muscle to reflect edible portions. From the muscle portion of these samples, specific sections measuring 3 × 2 × 1 cm (width × length × depth) were then collected from the injection site for histopathological analysis at 12, 24, 48, 72, 168, and 480 hpi. The overall experimental design is summarized schematically in Fig. 2.

Histopathological analysis

All samples were initially fixed in Bouin's solution (BBC, Mount Vernon, WA, USA) for 24 hours and then re-fixed in the same solution for 48 hours. The tissues were then immersed in 70% ethanol for 24 hours. Tissue processing—including dehydration, clearing, and paraffin infiltration—was performed using an automatic tissue processor (Leica TP 1020, Wetzlar, Germany). The processed tissues were embedded in paraffin, sectioned into 4–5 μm thick slices, and stained using Harris hematoxylin and eosin (H&E) solution (Leica, Teaneck, NJ, USA).

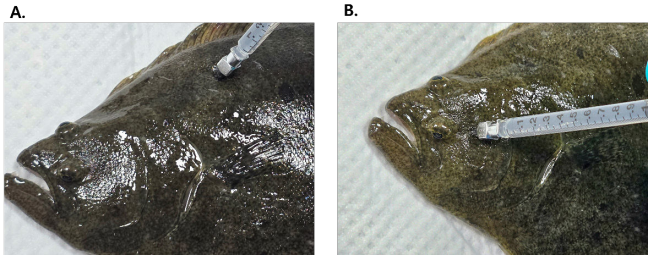

Fig. 1. Representative images illustrating the intramuscular injection sites for amoxicillin administration in olive flounder (*Paralichthys olivaceus*): (A) dorsal muscle, (B) cheek muscle.

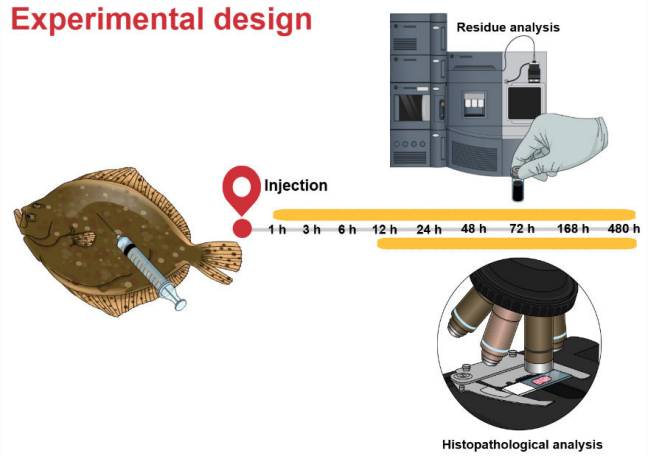

Fig. 2. Experimental design and sampling schedule for amoxicillin intramuscular injection in olive flounder.

Sample preparation and extraction

High-performance liquid chromatography (HPLC)-grade water and acetonitrile (J.T. Baker, Phillipsburg, NJ, USA) were used throughout all extraction and chromatographic procedures. Other reagents, including amoxicillin sodium (molecular weight 365.4), piperacillin (molecular weight 517.5), acetic acid, sodium phosphate dibasic (Na_2HPO_4), potassium dihydrogen phosphate (KH_2PO_4), and formic acid, were of analytical grade and obtained from Sigma-Aldrich (St. Louis, MO, USA). Solid-phase extraction (SPE) was performed using OASIS PRiME HLB cartridges (6 cc, 200 mg; Waters, Milford, MA, USA). For sample extraction, 2 g of homogenized tissue samples (muscle including skin) were placed into 50-mL conical polypropylene tubes. After adding 1 mL of 0.1 N acetic acid, the samples were subjected to sonication at 60 Hz and 300 W for 5 min at 25℃. Methanol (8 mL) and an internal standard (IS) solution (piperacillin, 500 ppb, 200 μL) were subsequently added, followed by centrifugation at 20,000×g for 10 min at 4℃. The supernatant was carefully transferred to 15-mL conical tubes and evaporated under a nitrogen stream at 50℃. The dried residue was reconstituted in 5 mL of 0.1 M Na_2HPO_4 (pH 7.2) and loaded onto preconditioned SPE cartridges. The cartridges were rinsed with 5 mL of 0.05 M Na_2HPO_4 and eluted with 5 mL of a 0.05 M KH_2PO_4 : Acetonitrile mixture (50:50, v/v). After evaporation of the eluate under nitrogen at 50℃, the final extract was dissolved in 1 mL of water and filtered using 0.2-μm polyvinylidene fluoride (PVDF) syringe filters prior to high-performance liquid chromatography–tandem mass spectrometry (HPLC)-MS/MS analysis.

High-performance liquid chromatography–tandem mass spectrometry (HPLC-MS/MS) conditions and method validation

Piperacillin was selected as the internal standard based on the guidelines of the Ministry of Food and Drug Safety (MFDS, 2023). It is a β-lactam antibiotic with similar extraction and ionization behavior to amoxicillin, and it is entirely absent endogenously in olive flounder tissue. The analytical method was validated with a limit of quantitation (LOQ) of 10 ng/mL for muscle matrices. The matrix-matched calibration curve exhibited excellent linearity across the range of 10–500 ng/mL. Inter-day precision, assessed at 1×, 5×, and 10× LOQ levels, demonstrated a coefficient of variation below 12.12%. Mean recovery rates ranged from 95.44% to 109.92%, ensuring a stable response consistent with the acceptance criteria outlined in the Bioanalytical Method Validation Guidance for Industry. Under the established chromatographic conditions, the retention times were 2.81 min for amoxicillin and 9.88 min for piperacillin (IS), demonstrating

https://doi.org/10.47853/FAS.2026.e52

successful baseline separation. Detailed HPLC-MS/MS analytical conditions are summarized in Table 1.

Pharmacokinetic and pharmacodynamic analysis

Pharmacokinetic parameters of amoxicillin in muscle tissue were determined using non-compartmental analysis (NCA) based on statistical moment theory, conducted with the PKSolver add-in program for Microsoft Excel (Zhang et al., 2010). The maximum concentration (C_{max}) and time to reach C_{max} (T_{max}) were obtained directly from the observed data. The area under the concentration–time curve (AUC) and the area under the first moment curve (AUMC) was calculated using the linear trapezoidal method. The terminal elimination rate constant (λ_z) was estimated by linear regression of the log-transformed concentration data, and the terminal half-life ($t_{1/2\lambda z}$) was calculated as ln 2 divided by λ_z. The mean residence time (MRT) was determined by dividing AUMC by AUC.

Table 1. Amoxicillin analysis conditions using HPLC-MS/MS

Condition	Content		
Instrument	Agilent 6430 triple quad detector (Agilent Technologies, Santa Clara, CA, USA)		
LC parameter			
Column	Waters XSelect HSS C18 (2.1 mm, 150 mm, 3.5 μm)		
Mobile phase	A: 0.05% formic acid in water		
	B: 0.05% formic acid in acetonitrile		
Gradient	Time (min)	A (%)	B (%)
	0	90	10
	10	50	50
	15	25	75
	15.1	90	10
	20	90	10
Flow rate	0.2 mL/min		
Oven temp.	35℃		
Injection volumn	10 μL		
Run time	20 min		
Post time	3 min		
MS/MS parameter			
Ionization	ESI, Positive		
Collision gas	N_2		
Gas temperature	350℃		
Retention time (min)	Amoxicillin	2.81	
	Piperacillin	9.88	
Scan type	Multiple reaction monitoring (MRM mode)		
		Precursor ions (m/z)	Fragment ions (m/z)	Collision energy (eV)
	Amoxicillin	366.2	349.0, 114.0	3, 20
	Piperacillin	518.2	160.1, 143.1	5, 30

HPLC-MS/MS, high-performance liquid chromatography–tandem mass spectrometry; LC parameter, liquid chromatography parameter; ESI, electrospray ionization.

Pharmacodynamic evaluations utilized minimum inhibitory concentration (MIC_{90}) values of 0.0312 μg/mL for *Streptococcus iniae* and 0.5 μg/mL for *Streptococcus parauberis*, adopted from published susceptibility datasets for clinical isolates from Korean olive flounder (Lim et al., 2017). Because MIC distributions may vary by region and time, these indices should be interpreted as exposure comparisons under the selected MIC_{90} scenario. Based on the concentration–time profiles in the muscle, PK/PD exposure indices including C_{max}/MIC_{90}, AUC/MIC_{90}, and the duration of time that concentrations exceeded MIC_{90} ($T > MIC_{90}$) were calculated. Because the tissue-specific free fraction (*f*u) of amoxicillin in fish muscle remains empirically undetermined, the total drug concentration was used; therefore, the index is expressed as $T > MIC_{90}$ (total). Since only the unbound drug is microbiologically active, particularly for time-dependent β-lactams like amoxicillin, these indices represent the upper bound of potential local antibacterial pressure.

It must be emphasized that no blood samples were collected, and serum PK parameters were not empirically evaluated in the present study. To provide a systemic baseline for therapeutic efficacy, we extracted the established serum PK profiles from a previous foundational study (Lee et al., 2023) conducted under identical dosing and environmental conditions. The PK/PD-related exposure indices in muscle obtained from the present study were calculated strictly to compare local tissue exposure and drug retention between injection sites, providing pharmacological evidence for injection-induced tissue damage, and were not intended to predict the clinical cure of systemic streptococcosis.

Results

Histopathological analysis

IM injection of amoxicillin induced distinct time-dependent histopathological changes in both the dorsal and cheek muscles at the injection sites. Representative histological lesions were consistently observed in both muscle groups, demonstrating a comparable pattern of tissue damage and recovery over time. At 12 hours post-injection, both dorsal and cheek muscles exhibited extensive hemorrhage, interstitial edema, myofiber atrophy, and necrosis. These findings indicate acute muscle injury occurring shortly after drug administration. By 24 and 48 hours,

edema and necrosis remained prominent, with fragmented myofibers and inflammatory cell infiltration becoming evident. At 72 hours, inflammation intensified and was accompanied by partial hyalinization and ongoing fragmentation of muscle fibers, suggesting ongoing tissue degeneration. By 168 hours, widespread and diffuse inflammatory infiltrates persisted in both groups, reflecting a sustained immune response. Even at 480 hours post-injection, histological examination revealed persistent interstitial edema and persistent atrophy of affected myofibers, with only partial resolution of inflammation. Overall, both the dorsal and cheek muscles demonstrated substantial damage following intramuscular administration of amoxicillin. Despite gradual reduction of hemorrhage and inflammatory activity over time, full histological recovery was not achieved within the 20-day observation period (Figs. 3 and 4).

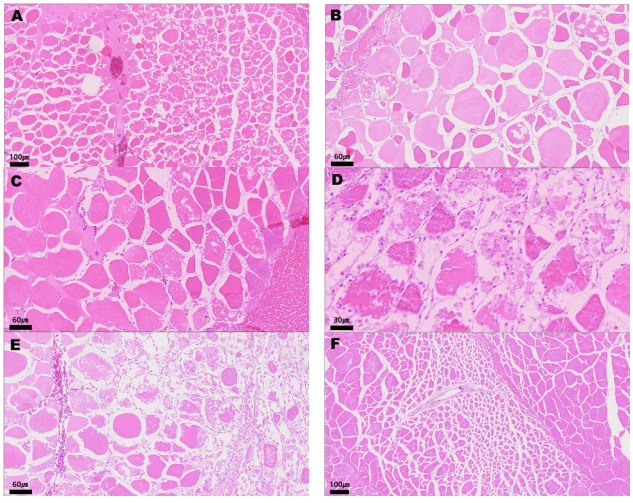

Fig. 3. Histopathological alterations in dorsal muscle following intramuscular administration of amoxicillin. (A) At 12 hours post-injection, hemorrhage, interstitial edema, myofiber atrophy, and extensive necrosis with severely fragmented muscle fibers are observed. Scale bar = 100 μm. (B) At 24 hours post-injection, edema and necrosis are present, with atrophic muscle fibers displaying a transition from angular to rounded shapes and hyper-eosinophilic sarcoplasm. Scale bar = 60 μm. (C) At 48 hours post-injection, edema, atrophy, and myofiber necrosis remain prominent. Scale bar = 60 μm. (D) At 72 hours post-injection, there is marked loss of muscle fibers, with inflammatory cell infiltration surrounding the muscle fibers, contributing to necrosis. Scale bar = 30 μm. (E) At 168 hours post-injection, widespread inflammatory infiltrates are observed within the dorsal muscle. Scale bar = 60 μm. (F) At 480 hours post-injection, edema and muscle fiber atrophy persist. Scale bar = 100 μm. Hematoxylin and eosin staining was used for all panels.

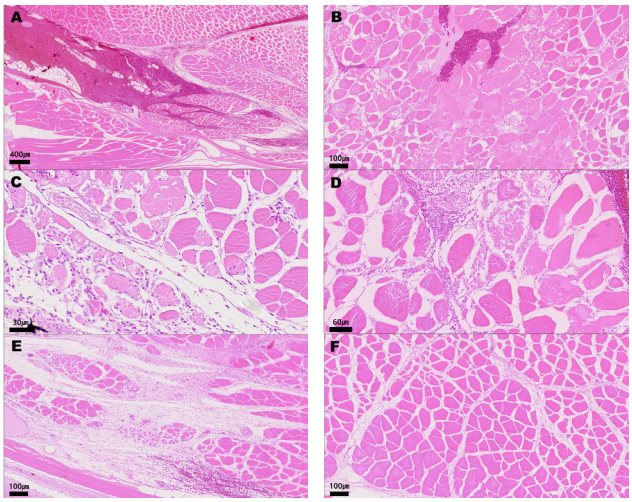

Fig. 4. Histopathological alterations in cheek muscle following intramuscular administration of amoxicillin. (A) At 12 hours post-injection, extensive hemorrhage is distributed throughout the muscle tissue. Scale bar = 400 μm. (B) At 24 hours post-injection, hemorrhage, interstitial edema with pale pink material, myofiber atrophy, and focal necrosis are observed. Scale bar = 100 μm. (C) At 48 hours post-injection, inflammatory cell infiltration is seen alongside distinct fragmentation of muscle fibers. Scale bar = 30 μm. (D) At 72 hours post-injection, fragmented and partially hyalinized muscle fibers are observed, accompanied by atrophy and inflammatory infiltration. Scale bar = 60 μm. (E) At 168 hours post-injection, widespread inflammatory infiltrates are diffusely distributed throughout the tissue. Scale bar = 100 μm. (F) At 480 hours post-injection, interstitial edema and myofiber atrophy remain. Scale bar = 100 μm. Hematoxylin and eosin staining was used for all panels.

Muscle concentration

Following intramuscular administration of amoxicillin sodium into the cheek and dorsal muscles of olive flounder, tissue concentrations of the drug were measured at multiple time points using HPLC–MS/MS (Fig. 5). Sampling was performed at 0.5, 1, 3, 6, 12, 24, 48, 72, 168, and 480 hours post-injection, with seven fish analyzed per time point. To visualize inter-individual variation, concentrations from all individuals were plotted as individual data points. Fig. 5A shows the comparative concentration–time profiles between the two injection sites, while Fig. 5B and 5C present individual profiles for the dorsal and cheek muscles, respectively, along with magnified views of the terminal phase, focusing on the decline below the maximum residue limit (MRL; 0.05 mg/kg).

In the cheek muscle group, amoxicillin was rapidly absorbed, reaching the peak concentration (C_{max}) at 3 hours, followed

https://doi.org/10.47853/FAS.2026.e52

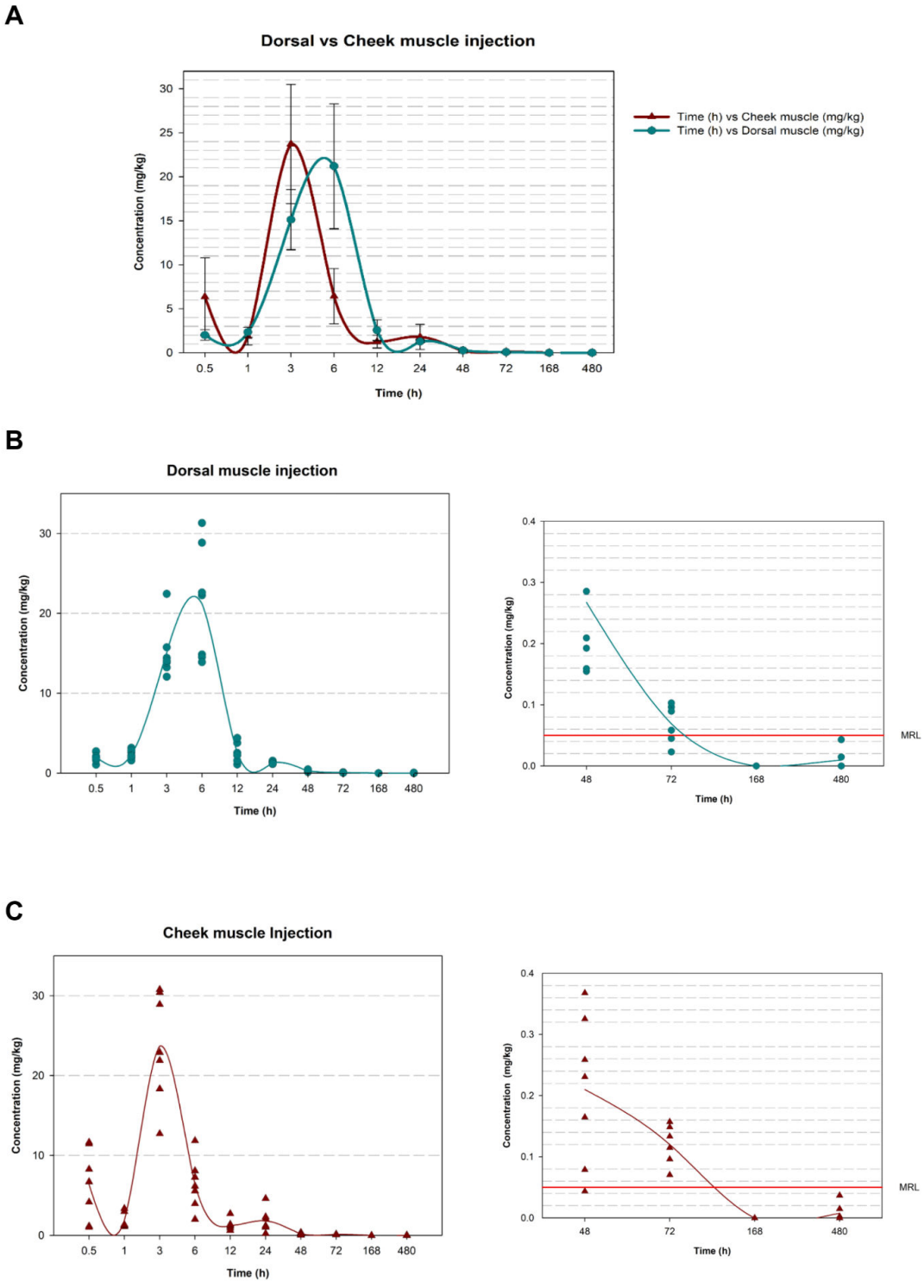

Fig. 5. Muscle residue depletion of amoxicillin after intramuscular injection in olive flounder. (A) Comparison of amoxicillin concentrations in muscle tissue after injection into the dorsal and cheek muscles. (B) Residue depletion profiles in dorsal muscle: full time course (left) and magnified view highlighting the point below the MRL (right). (C) Residue depletion profiles in cheek muscle: full time course (left) and magnified MRL comparison (right). The red dotted line indicates the MRL. Error bars represent SD. MRL, maximum residue limit.

by a sharp decline. In some individuals, a secondary rise in concentration was observed. In contrast, the dorsal muscle group exhibited a more gradual increase in drug concentration, with a relatively flattened terminal phase.

The rate at which the drug concentration declined below the MRL was faster in the dorsal muscle group, where most samples fell below the threshold after 168 hours. However, in the cheek muscle group, detectable concentrations near the MRL were still observed in a few individuals at 480 hours. Notably, greater inter-individual variability was observed in the cheek muscle group compared to the dorsal group, indicating higher variability in local absorption and/or distribution dynamics at that site.

Pharmacokinetic/pharmacodynamic relationships

Following the IM injection of amoxicillin into the dorsal or cheek muscle of olive flounder, distinct pharmacokinetic profiles were observed in the serum versus muscle compartments (Table 2). It should be noted that direct statistical comparisons between the two compartments were not performed because the serum parameters were derived from the literature (Lee et al., 2023), whereas the muscle parameters were obtained from the present *in vivo* study. All differences are described in terms of observed trends.

In the systemic circulation (serum data adapted from Lee et al., 2023), amoxicillin reached a high peak concentration (C_{max}) of approximately 203 μg/mL at 3 h post-injection for both the dorsal and cheek injection sites. Systemic exposure, as indicated by AUC_{0-t}, was robust in both groups, confirming that both injection sites provide sufficient systemic bioavailability for treating systemic infections.

In contrast, within the muscle tissue (present study), local drug absorption was generally slower and exhibited different kinetic patterns. The T_{max} values were 6 h and 3 h for the dorsal and cheek injections, respectively. The dorsal muscle group showed a higher local C_{max} (21.19 μg/mL) and AUC_{0-t} (207.91 μg/mL·h) than the cheek muscle group. Notably, the mean residence time MRT_{0-inf} in the muscle tissue was longer for the cheek injection (31.43 h) compared to the dorsal injection (23.08 h).

To evaluate the extent of local tissue exposure—which correlates with injection-site damage—PK/PD-related indices were calculated based on the total drug concentrations in the muscle. Against *S. iniae* (MIC_{90} = 0.0312 μg/mL) and *S. parauberis* (MIC_{90} = 0.5 μg/mL), the dorsal injection consistently produced higher local exposure indices (C_{max} / MIC_{90}, AUC_{0-t} / MIC_{90}, and T > MIC_{90} (total)) compared to the cheek injection. These findings indicate that while serum exposure is highly favorable for both sites (Lee et al., 2023), the dorsal muscle experiences a greater magnitude of local drug exposure, providing a pharmacological basis for the observed severe injection-induced tissue damage and the residue depletion patterns during the withdrawal period.

Table 2. Comparison of non-compartmental pharmacokinetic and pharmacokinetic/pharmacodynamic (PK/PD) parameters of amoxicillin in serum and muscle following intramuscular injection into dorsal and cheek muscles of olive flounder (*Paralichthys olivaceus*)

PK parameters	Unit	Serum		Muscle	
		Dorsal	Cheek	Dorsal	Cheek
Tmax	h-1	3.00	3.00	6.00	3.00
Cmax	μg/mL	202.79	203.96	21.19	17.67
AUC0-t	μg/mL·h	1,697.23	2,006.71	207.91	147.71
AUMC0-inf	μg/mL·h^2	24,469.78	24,582.22	4,799.11	4,642.85
MRT0-inf	h	14.34	12.11	23.08	31.43
PK/PD parameters					
Streptococcus iniae					
C_{max} / MIC_{90}		6,499.68	6,537.18	679.23	566.36
AUC_{0-t} / MIC_{90}		39,333.01	64,317.63	6,663.72	4,734.28
$AUMC_{0-inf}$ / MIC_{90}		54,398.40	65,044.55	153,817.79	148,809.22
T > MIC_{90}		111.61	132.37	124.14	137.83
Streptococcus parauberis					
C_{max} / MIC_{90}		405.58	407.92	42.38	35.34
AUC_{0-t} / MIC_{90}		3,394.46	4,013.42	415.82	295.42
$AUMC_{0-inf}$ / MIC_{90}		3,412.84	4,058.78	9,598.23	9,285.70
T > MIC_{90}		76.05	85.35	41.96	41.85

All PK/PD ratios were calculated using corresponding MIC_{90} values for each organism.
PK/PD indices were calculated using MIC_{90} values of 0.0312 μg/mL for *Streptococcus iniae* and 0.5 μg/mL for *Streptococcus parauberis*.
C_{max}, maximum observed concentration; T_{max}, time to reach C_{max}; AUC_{0-t}, area under the concentration–time curve from time zero to the last quantifiable concentration; $AUMC_{0-inf}$, area under the first moment curve extrapolated to infinity; MRT_{0-inf}, mean residence time extrapolated to infinity.
Serum PK parameters were based on data from Lee et al. (2023), while muscle parameters were derived from the present study using non-compartmental analysis.

Discussion

IM injection is widely recognized to cause muscle damage, including hemorrhage, inflammation, and tissue necrosis in terrestrial animals such as humans, cattle, and pigs (Abbate et al., 2018; Zoltick et al., 2024). To minimize these adverse effects, international organizations such as the World Health Organization (WHO) and Centers for Disease Control and Prevention (CDC)

https://doi.org/10.47853/FAS.2026.e52

have issued guidelines on safe injection practices (CDC, 2025; WHO, 2016). Despite these efforts, adverse tissue reactions continue to occur. For instance, in the swine industry, damaged muscle tissue at injection sites is routinely excised during slaughter to ensure food safety. In the Korea, although injection guidelines for farmed fish have been established, the recommended injection site is strictly limited to the anterior dorsal muscle between the dorsal fin and lateral line (Jeong, 2006). Unlike livestock processing, however, the removal of injection-site lesions is not standard practice in the seafood supply chain. Because this traditional dorsal injection site is a primary edible portion, persistent injection marks remain visible to end-consumers. Therefore, this study evaluated the cheek muscle, a non-edible anatomical site, as a practical alternative injection location.

Muscle damage from IM injection typically results from a combination of chemical drug toxicity, physical needle trauma, and the osmotic effects of the injected solution (Svendsen et al., 1998). Tissue recovery generally progresses through four stages: hemostasis, inflammation, proliferation, and remodeling (Velnar et al., 2009), a process that occurs similarly in teleost (Finn & Nielson, 1971). In the present study, all four stages of wound healing were evident at both the dorsal and cheek sites, beginning with initial hemorrhage, followed by extensive inflammation and necrosis, and eventually showing a gradual reduction in the inflammatory response. The recovery trajectories were macroscopically and microscopically similar over time between the two injection sites. However, even after the mandatory 20-day withdrawal period, the tissues remained in the proliferation and remodeling stages, and complete histological recovery was not achieved. This critical finding suggests that current statutory withdrawal periods, which are established solely based on drug elimination kinetics from edible tissues, may be insufficient to ensure complete physiological recovery from injection-induced trauma.

Because the histopathological analysis revealed no significant differences in the severity of tissue damage between the cheek and dorsal muscles, the site-specific muscle residue depletion and pharmacokinetic profiles were comparatively analyzed to understand the local drug dynamics. The analysis revealed distinct kinetic differences: the cheek muscle group reached its maximum local concentration (C_{max}) rapidly at 3 hours post-administration, followed by a sharp decline, whereas the dorsal muscle group exhibited a slower rise and a prolonged elimination phase. These differences likely reflect the anatomical and physiological characteristics of the cheek muscle, which possesses a richer vascular supply compared to the dorsal musculature, facilitating more rapid drug absorption and distribution into the systemic circulation. Notably, the cheek muscle group exhibited substantial inter-individual variability, with secondary concentration peaks observed in several individuals. This variability suggests potential drug redistribution or delayed absorption mediated by the specific anatomical confines of the buccal cavity. Furthermore, some individuals in the cheek group maintained detectable concentrations near the MRL up to 480 hours, underscoring the necessity for robust safety assessments that account for high inter-individual variations in alternative injection sites.

As this study was designed as a direct experimental extension of Lee et al. (2023)—utilizing olive flounder from the same farm and batch under identical dosing and environmental conditions—their serum PK/PD data serve as a scientifically robust systemic reference. Regarding the pharmacokinetic/pharmacodynamic (PK/PD) relationships, a clear distinction must be made between systemic therapeutic efficacy and local tissue exposure. As previously established by Lee et al. (2023), cheek muscle injection yields comparable or superior serum PK/PD indices against *S. iniae* and *S. parauberis* compared to dorsal injection, ensuring sufficient systemic exposure to eradicate these pathogens. However, our current muscle-specific PK/PD analysis revealed a different dynamic at the local level. The dorsal muscle injection resulted in higher local exposure indices ($AUC_{0\text{-}t}$ / MIC_{90} and $T > MIC_{90}$) within the muscle tissue itself. This heightened and prolonged local drug retention in the dorsal muscle provides a pharmacological rationale for the sustained tissue damage observed in this study. Thus, while both sites are viable for delivering systemic therapy, transitioning to the non-edible cheek muscle offers the distinct advantage of isolating this inevitable local tissue damage away from the economically valuable fillet.

Several methodological limitations of this study should be acknowledged. First, a sham-injected (PBS/saline) control group was not included. However, a previous study evaluating intramuscular injections in olive flounder demonstrated that the administration of PBS alone does not induce significant or prolonged histopathological alterations at the injection site (Joo et al., 2020). Therefore, while the exact relative contributions of mechanical needle trauma versus amoxicillin-specific cytotoxicity cannot be perfectly isolated, the extensive, severe, and persistent tissue damage observed in our study is highly likely driven primarily by the chemical toxicity of the

amoxicillin formulation itself. Second, because the specific free fraction (protein binding rate) of amoxicillin in fish tissue has not been empirically determined, the PK/PD indices (such as $T > MIC_{90}$) were calculated based on total drug concentrations. As the antibacterial efficacy of beta-lactams is primarily driven by the free drug fraction ($fT > MIC$) (Cars, 1997), this may overestimate the active drug exposure. If amoxicillin exhibits significant protein or tissue binding in olive flounder muscle, the actual $fT > MIC_{90}$ would be lower than reported here, potentially overestimating the local antibacterial pressure at the injection site. Furthermore, the degree of overestimation may differ between the dorsal and cheek muscle compartments if tissue-specific binding varies between sites; therefore, the PK/PD indices reported here should be interpreted strictly as relative comparisons of local drug retention rather than absolute predictors of antibacterial efficacy. While the use of a synchronized batch significantly reduces inter-group variability, inherent individual physiological differences in drug absorption and distribution cannot be entirely discounted, which may introduce a degree of imprecision in the direct cross-compartment comparison. Finally, this study was conducted using healthy individuals, which may not fully capture the pharmacokinetic alterations that occur during actual diseased states. Future research should focus on the standardization of alternative injection techniques, evaluation under clinical infection scenarios, and the determination of specific protein binding profiles in teleost.

Conclusion

This study evaluated the clinical applicability of the cheek muscle as an alternative to the conventional dorsal injection site by comparing amoxicillin residue depletion patterns and histopathological changes in olive flounder. As an extension of the systemic pharmacokinetic framework established by Lee et al. (2023), this work elucidates the local tissue dynamics and physical consequences occurring directly at the injection sites. Our findings demonstrate that while the statutory 20-day withdrawal period is sufficient for drug elimination below the MRL, it does not guarantee complete histological recovery from injection-induced trauma. Therefore, transitioning to a non-edible administration site such as the cheek muscle offers a highly practical solution to preserve fillet quality and consumer confidence without compromising systemic therapeutic efficacy. To establish comprehensive, evidence-based recommendations for aquaculture medicine, future investigations must explore standardized injection protocols, multi-species applications, and the pharmacokinetic impacts of diseased states.

Competing interests

No potential conflict of interest relevant to this article was reported.

Funding sources

This research was supported by the National Fisheries Products Quality Management Service (NFQS) grant (Grant No. NFQS2025002).

Acknowledgements

Not applicable.

Availability of data and materials

Upon reasonable request, the datasets used in this study can be available from the corresponding author.

Ethics approval and consent to participate

All fish experiments were approved by the Institutional Animal Care and Use Committee (IACUC, NFQS-2022-6).

ORCID

Ga-Won Kim	https://orcid.org/0009-0000-7474-0296
Hyo-Eun Lee	https://orcid.org/0000-0002-0892-3374
Joo-Won Hong	https://orcid.org/0009-0001-8200-6953
Mun-Gyeong Kwon	https://orcid.org/0000-0003-4263-9702
Ji-Hoon Lee	https://orcid.org/0000-0001-5974-1872
Jung-Soo Seo	https://orcid.org/0009-0009-6923-1249

References

Abbate A, Almasio PL, Mongitore M, Di Vita G, Patti R. Necrotizing soft tissue fasciitis after intramuscular injection. Case Rep Surg. 2018;2018:3945497.

Cars O. Efficacy of beta-lactam antibiotics: integration of pharmacokinetics and pharmacodynamics. Diagn Microbiol Infect Dis. 1997;27:29-33.

Centers for Disease Control and Prevention (CDC). Vaccine administration: intramuscular (IM) injection: adults 19 years of age and older [Internet]. CDC. 2025. https://www.cdc.gov/vaccines/hcp/admin/downloads/IM-injection-adult.pdf

https://doi.org/10.47853/FAS.2026.e52

Finn JP, Nielson NO. The inflammatory response of rainbow trout. J Fish Biol. 1971;3:463-78.

Food and Agriculture Organization of the United Nations (FAO). The state of world fisheries and aquaculture 2024. Rome: FAO; 2024.

Jeong TS. Current status of usage and reduction measures for fishery antibiotics. J Korean Vet Med Assoc. 2006;42:63-71.

Joo MS, Hwang SD, Choi KM, Kim YJ, Hwang JY, Kwon MG, et al. Application of tylosin antibiotics to olive flounder (*Paralichthys olivaceus*) infected with *Streptococcus parauberis*. Fis Aquat Sci. 2020;23:20.

Kim Y, Seo J, Park J, Jeong AR, Lee J. Monitoring of aquatic medicine managements in South Korea. J Fish Pathol. 2019;32:37-43.

Ko BS. Collapse of clean image due to antibiotic marks in Jeju olive flounder… Consumer boycott shifts favor to Wando [Internet]. International News. 2023. https://www.gukjenews.com/news/articleView.html?idxno=1131617

Krkošek M. Host density thresholds and disease control for fisheries and aquaculture. Aquac Environ Interact. 2010;1:21-32.

Lee JH, Kim GW, Kang HW, Hong JW, Lee HE, Kwon MG, et al. Influence of intramuscular injection sites on pharmacokinetics of amoxicillin in olive flounder (*Paralichthys olivaceus*) and its implication for antibacterial efficacy. Pharmaceutics. 2023;15:1153.

Lim JW, Jung MH, Jung SJ, Kim DH, Park KH, Kang SY. The efficacy of amoxicillin sodium against streptococcosis in cultured olive flounder *Paralichthys olivaceus* and its pharmacokinetics. J Vet Pharmacol Ther. 2017;40:77-87.

Ministry of Food and Drug Safety (MFDS). Maximum residue limits for veterinary drugs [Internet]. MFDS. 2023. https://residue.foodsafetykorea.go.kr/vd/mrl

National Fishery Products Quality Management Service (NFQS). Pharmacist handbook [Internet]. NFQS. 2025. https://www.nfqs.go.kr/apms/search/goodsList.ad

Park TW. Export slump and boycott… Olive flounder continues to plummet [Internet]. Busan Ilbo. 2019. https://www.busan.com/view/busan/view.php?code=20190618000070

Statistics Korea. Preliminary results of the survey on the status of fish culture in 2024 [Internet]. Statistics Korea. 2025. https://https://kosis.kr/statHtml/statHtml.do?sso=ok&returnurl=https%3A%2F%2Fkosis.kr%3A443%2FstatHtml%2FstatHtml.do%3Fconn_path%3DI2%26tblId%3DDT_1EZ0008%26orgId%3D101%26

Svendsen O, Hansen HB, Jørgensen KD. Significance of injection solution temperature on local muscle tissue damage in pigs. Pharmacol Toxicol. 1998;82:301-3.

Velnar T, Bailey T, Smrkolj V. The wound healing process: an overview of the cellular and molecular mechanisms. J Int Med Res. 2009;37:1528-42.

World Health Organization (WHO). WHO guideline on the use of safety-engineered syringes for intramuscular, intradermal and subcutaneous injections in health care settings. Geneva: WHO; 2016.

Zhang Y, Huo M, Zhou J, Xie S. PKSolver: an add-in program for pharmacokinetic and pharmacodynamic data analysis in Microsoft Excel. Comput Methods Programs Biomed. 2010;99:306-14.

Zoltick AH, Mann S, Coetzee JF. Pain pathophysiology and pharmacology of cattle: how improved understanding can enhance pain prevention, mitigation, and welfare. Front Pain Res. 2024;5:1396992.